ROYAL SOCIETY OF CHEMISTRY

PAPER

Check for updates

Methanolysis of polyethylene terephthalate (PET) using non-stoichiometric protic ionic liquids

Emma McCrea, [ID] Peter Goodrich, John D. Holbrey [ID] and Małgorzata Swadźba-Kwaśny [ID] *

Methanolysis of polyethylene terephthalate (PET) to dimethyl terephthalate (DMT), carried out in a microwave reactor, was catalysed by an inexpensive and recyclable non-stoichiometric protic ionic liquid, formulated from sulfuric acid and triethylamine. The influence of the catalyst composition (excess of acid or base), reaction temperature and time, as well as methanol excess, on the conversion of PET and the yield of DMT, was investigated. Under optimised conditions (3 h, 180 °C), waste PET from milled plastic bottles was depolymerised, reaching 100% PET conversion and 98% isolated yield of DMT. Pure DMT was separated through recrystallisation directly from the reaction mixture. Preliminary experiments with carpet waste (dyed mixed polymer waste, without milling) gave results on par with those achieved for PET bottles, with 100% PET conversion and 97% of DMT (isolated yield).

Sustainability spotlight

This work addresses the need for an economically viable PET depolymerisation process, catalysed by an inexpensive and reusable protic ionic liquid. It handles contaminated waste (dyed carpets) without preprocessing and enables closed-loop recycling by producing a virgin-quality PET monomer, dimethyl terephthalate. The process contributes to truly circular PET recycling (SDG12 – sustainable consumption and production). Addressing plastic pollution promotes cleaner waters (SDG14 – life below water) and decreases landfill waste (SDG11 – sustainable cities and communities).

Introduction

Polyethylene terephthalate (PET) is one of the most widely used plastics, commonly found in beverage bottles and garments. While PET is often regarded as easily recyclable through mechanical processes, the reality falls short: in 2022, only 30% of PET bottles in the UK were recycled, and an even smaller fraction of PET-based garments underwent recycling.[1] Compounding the issue, approximately 75% of PET collected for recycling is rejected before reaching the processing stage. Of the remaining 25%, only 17% is recycled back into bottles, while over 50% is downcycled into fibres, which are themselves rarely recycled.[2,3] As a result, a truly closed-loop recycling system for PET remains elusive.

Although mechanical recycling plays a crucial role in extending the life cycle of plastics, it progressively degrades the quality of the material. In contrast, chemical recycling offers a more sustainable alternative by depolymerising PET into its original monomers. These building blocks can then be re-polymerised into high-quality PET, equivalent to its virgin counterpart.

Conventionally, PET is synthesised *via* polycondensation reactions between terephthalic acid (TPA) and ethylene glycol (EG) through direct esterification (Scheme 1a), or between dimethyl terephthalate (DMT) and EG *via* transesterification (Scheme 1b). Consequently, PET recycling can be achieved by reversing these reactions. Specifically, the ester bond in PET can be cleaved through methods such as methanolysis, glycolysis, hydrolysis, pyrolysis, aminolysis, or ammonolysis.[4,5] Among these, glycolysis is the most prevalent, producing bis(2-hydroxyethyl) terephthalate (BHET), a key intermediate for PET synthesis (Scheme 2a). Despite its high energy demand and complex purification steps, glycolysis remains attractive due to
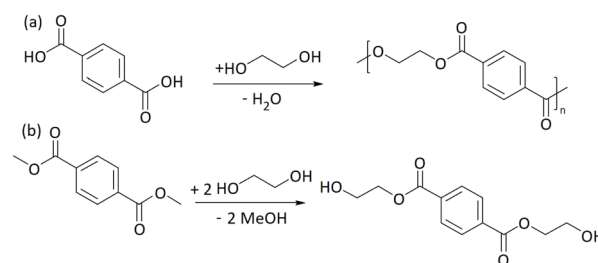
Scheme 1 Polycondensation of TPA and ethylene glycol *via* direct esterification (a); polycondensation of dimethyl terephthalate and ethylene glycol *via* transesterification (b).

The QUILL Research Centre, School of Chemistry and Chemical Engineering, Queen's University Belfast, Belfast BT9 5AG, UK. E-mail: m.swadzba-kwasny@qub.ac.uk
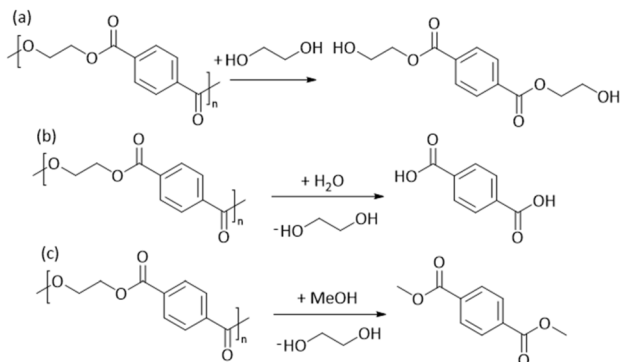
Scheme 2 Glycolysis of PET to BHET (a); hydrolysis of PET to TPA (b); methanolysis of PET to DMT (c).

the direct reusability of BHET.[6–13] Hydrolysis, in contrast, decomposes PET into TPA and EG (Scheme 2b) under acidic, basic, or neutral conditions. However, this method requires corrosion-resistant equipment, increasing capital expenditures and limiting its commercial appeal.[14–18] In comparison, methanolysis yielding DMT and EG (Scheme 2c) offers advantages in terms of easier product separation and purification.

Historically, methanolysis was first reported in the 1960s by Gruschke and co-workers, who developed a two-stage catalyst-free process involving PET melting (265–285 °C) followed by reaction with excess hot methanol under high pressure (30–40 atm) to produce pure DMT.[19] Building on this, Eastman Kodak patented a process in the 1990s using zinc acetate as a catalyst in either batch or continuous flow systems, operating with methanol or a methanol/glycol mixture at a PET : methanol molar ratio of 1 : 7–1 : 20.[20] Today, commercial methanolysis processes typically use PET flakes at 180–280 °C and 2–4 MPa.[21] However, these harsh conditions increase side reactions, including PET degradation to acetaldehyde, formaldehyde, and CO_2, as well as the partial ester exchange with methanol. Moreover, decomposition of EG to glyoxal and formic acid further compromises process efficiency, driving the search for milder and more efficient alternatives.

One such alternative is methanolysis using supercritical methanol, which offers near-complete PET conversion and a 95% DMT yield. Nonetheless, the extreme conditions required (260–270 °C, 9–11 MPa) result in high energy demands and elevated carbon emissions, limiting its commercial viability.[22,23]

To improve efficiency, catalytic methanolysis is commonly employed, typically with basic or acidic catalysts. In both cases, the ester bond is broken *via* nucleophilic substitution, where methanol's –OCH_3 group attacks the carbonyl carbon of the ester linkage, forming EG and DMT (Scheme 2c). Basic catalysts enhance this process by activating methanol for stronger nucleophilic attack, while Brønsted acids protonate the ester oxygen to increase electrophilicity.[24] Acidic catalysis often results in higher selectivity for DMT and better compatibility with contaminated PET waste.[25,44]

Recent patents reflect this trend. A 2021 patent granted to Eastman describes a catalytic process for PET methanolysis, using sodium carbonate, magnesium methoxide, 1,8-

diazabicyclo[5.4.0]undec-7-ene (DBU) and triazabicyclodecene (TBC) as chosen catalysts.[26] Other methods rely on basic, heterogeneous catalysts, such as sodium silicate,[27] potassium carbonate,[28] metal oxides and metal acetates, *e.g.* ZnO or $Zn(OAc)_2$, as well as metal hydroxides.[29] Although these catalysts accelerate the reaction, increase the conversion and the yield of DMT, they also have disadvantages. They lack selectivity to DMT, increasing the rate of side product formation alongside the targeted reaction, necessitating additional purification steps. Furthermore, metal catalysts cause fouling and leach into the product, resulting in discolouration of the recycled plastic.[13,29–31]

Muangmeesri *et al.* introduced an organocatalytic methanolysis process employing triethylamine to selectively depolymerise PET into high-purity dimethyl terephthalate (DMT) and ethylene glycol (EG) under milder conditions (200 °C, 2 h) with a reduced solvent-to-substrate ratio. Notably, this method allows efficient catalyst and solvent recirculation, minimising waste and energy input. Extending its versatility, the approach is applicable to other polyesters and polycotton textiles, yielding recoverable cotton suitable for viscose fiber production. However, when comparing product yield from polyester to polycotton material, the yield of DMT drops from 88% to 56% indicating that there is a reduced reactivity to the system when using mixed feedstock systems. A comprehensive life cycle assessment (LCA) indicates a net reduction of 1.88 kg CO_2-equivalent emissions per kg of PET recycled, outperforming incineration and conventional recycling processes. This work establishes a scalable, low-impact strategy for closed-loop recycling of PET and blended textile waste.[32]

In response to these limitations, ionic liquid-based approaches take advantage of their low vapour pressure and the ability to solubilise a broad range of polymers. For instance, lanthanide-containing ionic liquids (ILs) were used for the glycolysis of PET, showing cooperativity between imidazolium and phosphonium ILs with basic (chloride and acetate) anions, and lanthanide salts of the general formula $LnCl_3 \cdot xH_2O$, where Ln = La, Sm, Gd, Y, or Tm ($x = 6$ or 7). This was evidenced by the increase in BHET yield compared to that of the ionic liquid without the lanthanide salt.[12] Poly(ionic liquid)s synthesised from 1-vinyl-3-ethylimidazole acetate and acrylic acid zinc salts formed Pil-Zn^{2+} and achieved 100% PET conversion and 89% yield of DMT at relatively low temperature (170 °C). Pil-Zn^{2+} facilitates the activation of the ester bond, making the PET chain more susceptible to nucleophilic attack, which allows for milder conditions and minimises potential side reactions.[33]

Organocatalytic approaches have also demonstrated potential. For example, 1,3-dimethylimidazolium-2-carboxylate, [C_1mim-CO_2], and 1,3-dimethylimidazolium acetate, [C_1mim][OAc], were compared in a study of PET glycolysis. Basicity was found to be the deciding factor, and [C_1mim-CO_2] was more effective, as it works through N-heterocyclic carbene, which is a very strong base.[8]

Similarly, basic deep eutectic solvents (DESs), such as a combination of 1,5-diazabicyclo [4.3.0]-5-nonene (DBN) and phenol, also gave excellent results. The strong hydrogen-bonding network between the DES and the PET activates the

Paper

ester bond and increases the nucleophilicity of methanol. The interactions stabilise the transition state and improve the kinetics, leading to rapid depolymerisation under milder conditions and lower energy barriers (100% conversion and 95.3% DMT yield at 130 °C in 1 h).[34]

In the context of hydrolysis, sulfonic acid-functionalised Brønsted acidic ILs have been used for the hydrolysis of PET using 1-(3-propylsulfonic)-3-methylimidazolium chloride, [PSMIM]Cl. This catalyst was more effective than the benchmark (sulfuric acid), as the IL is understood to have greater hydrogen bonding interactions with PET, facilitating the depolymerisation (94% yield of TPA with 100% conversion at 210 °C over 24 h).[35]

A representative comparison of PET alcoholysis and hydrolysis processes is shown in Table 1, comparing reaction conditions and results.

While there are many IL-based systems that offer good yields and conversions under mild conditions, the key consideration is the high cost. Superbases such as DBU or sulfonic acid-functionalised ILs, although highly efficient, are significantly more expensive than conventional basic catalysts or thermal methods, thereby impacting the economic viability of their large-scale implementation.

Considering this, the present work investigates an economical alternative: a non-stoichiometric protic ionic liquid as a catalyst for PET methanolysis. Our group has previously explored protic ILs based on sulfuric acid and inexpensive amines, formulated with excess H_2SO_4.[36] These ILs demonstrated superior catalytic performance in esterification and Beckmann rearrangement reactions due to their favourable phase behaviour.[37,38] Building on this foundation, we now assess the efficacy of these ILs across various compositional ranges, as either acid- or base-rich systems for catalysing the methanolysis of PET.

Experimental

Materials

Methanol (≥99.8%) was purchased from Sigma-Aldrich and dried using 3 Å molecular sieves prior to use. Reagents and solvents used for product recrystallisation and analysis, such as deuterated chloroform and dichloromethane (DCM), were all analytical grade (≥99.8%), obtained from Sigma-Aldrich, and used as received.

Polyethylene terephthalate (PET) was sourced from commercially available water bottles, washed with detergent, and dried before use. Carpet samples (dyed PET with latex backing) were sourced from a commercial carpet supplier.

Synthesis of ionic liquids

The ionic liquids were synthesised using a literature procedure.[33,34] In a typical experiment, sulfuric acid (1 mol eq.) was placed in a round-bottom flask with a magnetic stirrer bar and cooled in an ice bath with vigorous stirring (400 rpm). The base (0.5–2 mol eq.) was added dropwise and left to react (70 °C, 1 h, 400 rpm). The products were dried under reduced pressure at 40 °C for 12 h and stored over argon to prevent moisture absorption.

Methanolysis of PET

PET was ground using a ball mill (Retsch MM400, 30 Hz, 12 h) to a uniform powder (40–60 mesh sieve, 400–250 μm). Subsequently, a sample of PET (0.0025–0.005 mol) was placed in

Table 1 Comparison of selected PET alcoholysis and hydrolysis processes

Catalyst	Solvent	Temperature (°C)	Pressure (atm)	Time (h)	Conversion of PET (%)	Yield of DMT (%)	Ref.
None	Methanol	265–285 °C	30–40		99	99	19
Zn(OAc)$_2$	Methanol for batch Methanol and alkylene glycols	240–260	24–40	2–6	95	85–90	20
[Bmim][BF$_4$]	Supercritical ethanol	240	64	0.75	98	97 (diethylterephthalate)	22
DBU	Methanol	140	1–15	4	90	75	23
TBD	Methanol	140	1–15	4	88	70	23
NaOMe	Methanol	110	1–15	4	81	62	23
Na$_2$CO$_2$	Methanol	140	1–15	4	99	77	23
Mg(OMe)$_2$	Methanol	180	1–15	4	99	80	23
MgO-modified NaY zeolite	Methanol	220	1	3	95	85	24
N$_{222}$	Methanol	180	1	4	99	88	25
Zn(OAc)$_2$	Methanol	200	1	1	99	98	26
[C$_4$mim]Cl with CeCl$_3$	Ethylene glycol	200	Autogenous	4	95	85 (BHET)	12
[C$_1$mim-CO$_2$]	Ethylene glycol	185	1	3	100	60 (BHET)	8
DBN and phenol	Methanol	130	1	1	100	95	29
[PSMIM]Cl	Water	210	Autogenous	24	100	94 (TPA)	30
Al[OCH(CH$_3$)$_2$]$_3$	Methanol	200	20–40	2	96	64	23
Pil-Zn^{2+}	Methanol	170	Autogenous	1	100	90	33
N$_{222}$	Methanol, toluene	200	Autogenous	2	100	88	32

a 30 ml microwave vial equipped with a stirrer bar. Methanol (0.15 mol) and ionic liquid (0.01 mol) were added, the vial was sealed and placed in an Anton Paar Monowave 400 microwave reactor. Reactions were carried out at 100–180 °C for 0.25–6 h. Upon completion, the reaction mixture was cooled to 100 °C and two aliquots (2 × 1 ml) were removed from the reaction mixture for analysis by GC-MS and NMR spectroscopy.

Subsequently, the hot reaction mixture, including the unreacted solid PET, was transferred to a centrifuge vial (15 ml) and centrifuged using an Eppendorf Centrifuge 5702 (4000 rpm, 3 min). Unreacted PET was separated by vacuum filtration. *Note:* The reaction mixture must remain above 70 °C to ensure that DMT does not precipitate out before the vacuum filtration of unreacted PET. Separated PET was subsequently dried under vacuum (40 °C, 0.5 h) to constant mass, which was recorded.

The filtrate was transferred to a round-bottomed flask and placed in an acetone-dry ice bath (−78 °C, 1 h) to crystallise the product. The white, needle-like crystals were separated by vacuum filtration, washed with cold methanol (3 × 100 ml), and dried in air to constant mass, which was recorded.

Representative analysis of isolated DMT are shown in Fig. S2 (^{1}H NMR spectrum), Fig. S3 (GC-MS chromatogram), Fig. S4 and S5 (TGA measured curves) and Fig. S6 (FT-IR spectra).

Conversion of PET was determined using eqn (1), where $m_{\text{PET ini}}$ is the mass of PET used for the reaction and $m_{\text{PET fin}}$ is the mass of PET after the reaction.

$$\text{PET conversion } (\%) = \frac{m_{\text{PET ini}} - m_{\text{PET fin}}}{m_{\text{PET ini}}} \times 100\%. \quad (1)$$

Yield of DMT was calculated using eqn (2), where $n_{\text{DMT exp}}$ is the quantity of DMT measured or isolated (in moles) and $n_{\text{DMT theor}}$ is the theoretical quantity of DMT assuming complete conversion of PET.

$$\text{DMT yield } (\%) = \frac{n_{\text{DMT exp}}}{n_{\text{DMT theor}}} \times 100\%. \quad (2)$$

Selectivity of DMT was calculated using eqn (3), where $n_{\text{DMT iso}}$ is the quantity of DMT measured or isolated and n_{total} is the total quantity of all measured or isolated products.

$$\text{DMT selectivity } (\%) = \frac{n_{\text{DMT iso}}}{n_{\text{total}}} \times 100\%. \quad (3)$$

Methanolysis of the PET carpet sample

PET carpet with a latex backing was used to test the [HN$_{222}$·N$_{222}$][HSO$_4$] catalyst. The carpet was cut into small pieces with scissors and weighed. PET fibres were separated from the latex backing to determine PET content (0.0025 mol) and then recombined. The samples were placed in a reaction vessel equipped with a PTFE stirrer bar, with a high PET : methanol ratio (0.15 mol) and [HN$_{222}$·N$_{222}$][HSO$_4$] (0.01 mol), and heated at 180 °C for 3 h in an Anton Paar Monowave 400 microwave reactor. Product yield was calculated based on the initial moles of PET and analysed by GC-MS and ^{1}H NMR to assess the purity of the product.

Mass balance experiments

The methanolysis reaction was carried out according to the general procedure described. The mass balance experiment reuses the ionic liquid for 5 cycles with both low and high PET : methanol ratios. After removal of DMT by recrystallisation, the methanol-rich filtrate was transferred to a round-bottomed flask and removed under reduced pressure using a rotary evaporator until a constant mass was achieved. The resulting residue was treated with ethyl acetate and shaken to extract side products from the reaction mixture. Water was added, and the biphasic mixture was centrifuged to facilitate phase separation. The upper organic layer was removed. The aqueous layer was dried under vacuum on a Schlenk line overnight at 40 °C, followed by 60 °C, to remove ethylene glycol. The mass of each component was recorded at each stage. Representative mass balance data are shown in Tables S1 and S2, and ^{1}H NMR spectra of isolated ethylene glycol and ethyl acetate layers are provided in Fig. S27–S29.

GC-MS analysis

Before analysis, acids in the reaction mixture were derivatised using N,O-bis(trimethylsilyl)trifluoroacetamide (BSTFA). An aliquot of the reaction mixture was placed in a glass vial with a magnetic stir bar, and BSTFA was added in excess to the sample (1 : 10 ratio by volume). The mixture was allowed to react (60 °C, 400 rpm, 30 min) to ensure complete derivatisation. The reaction mixture was then allowed to cool and was diluted with DCM (1 : 7 ratio by volume). Finally, the solution was filtered with a 0.22 μm syringe filter to remove any particulates from entering the column and placed in a GC vial.

A sample (1 μL) was injected into an Agilent 8890 GC system, equipped with a 5977B GC/MSD detector and an HP-5MS UI (60–325 °C) 30 m × 250 μm × 0.25 μm column, using a post-column splitter with He carrier gas and split tubing (2.3 m × 150 μm internal diameter) to the MSD and to the front detector FID with an MSD transfer line temperature of 280 °C under the following conditions: helium (1.0 ml min^{-1}) as the carrier gas and injection with a 10 : 1 split ratio at 250 °C.

The oven temperature program was 50 °C (2 min hold), ramped at 10 °C min^{-1} to 250 °C (5 min hold), followed by a post-run at 300 °C (2 min). Mass spectrometric detection was performed in electron ionisation (EI) mode at 70 eV with a scan range of 50–500 *m/z*. The ion source and quadrupole temperatures were 230 °C and 150 °C, respectively. Data were acquired in full-scan mode for the identification and quantification of methanolysis products. DMT, EG, TPA, BHET, mono(2-hydroxyethyl) terephthalate (MHET), and monomethyl terephthalate (MMT) were quantified using five-point calibration curves (Fig. S8–S12).

NMR spectroscopic analysis

The purity and structure of the synthesised ionic liquids, [HN$_{222}$·N$_{222}$][HSO$_4$], [HN$_{222}$][HSO$_4$], and [HN$_{222}$][HSO$_4$]·H$_2$SO$_4$, were confirmed by ^{1}H and ^{13}C NMR spectroscopy using a Bruker AVANCE 400 MHz spectrometer. The samples were dissolved in

deuterated chloroform ($CDCl_3$). For quantitative NMR (qNMR), 1,3,5-trimethoxybenzene (0.1 g) was added as an internal standard prior to the reaction. The ^1H qNMR spectra were recorded with 32 scans and a relaxation delay of 5 seconds, while the ionic liquid samples were analysed with 16 scans and a 1-second relaxation delay. The internal standard was only used in the qNMR experiments (Fig. S13–S21). Upon completion of the reaction and before any separation, a known mass of the crude reaction mixture was dissolved in $CDCl_3$. ^1H NMR spectra were recorded at 400 MHz with 16 scans, and ^{13}C NMR spectra were recorded at 100.6 MHz with 128 scans (Fig. S1, S22, and S23, SI). ^1H NMR (400 MHz, $CDCl_3$ δ/ppm) [$HN_{222} \cdot N_{222}$][HSO_4]: 1.34 (t, J = 7.2 Hz 9H –CH_3), 2.17 (s 1H –NH), 3.16 (q 6H –CH_2–), 3.47 (s 10H N–CH_2–CH_3), 9.83 (s 1H –OH), ^{13}C NMR (100.6 MHz, $CDCl_3$ δ/ppm), 8.56 (C–CH_3), 46.18 (N–CH_2), 50.68 (N–CH_2).

The acceptor numbers of the three ionic liquid compositions were determined via ^{31}P NMR spectroscopy. All sample preparation was conducted under an inert atmosphere in a glovebox. Each ionic liquid (1.00 g) was weighed into a 10 cm^3 vial containing a PTFE-coated magnetic stir bar. Triethylphosphine oxide (TEPO, 1 mol%) was then added as the probe molecule for acceptor number measurement. Following the addition, the vials were sealed and stirred overnight to ensure complete dissolution of TEPO. After equilibration, the mixtures were transferred to 5 mm borosilicate NMR tubes containing sealed capillaries of deuterated dimethyl sulfoxide as a field lock. NMR tubes were sealed with parafilm and removed from the glovebox prior to analysis. ^{31}P NMR spectra were recorded on a Bruker AVANCE 400 MHz spectrometer at 60 °C. Chemical shifts were referenced externally to 85% H_3PO_4 in water. For comparison, TEPO solutions in hexane (1 mol%) were prepared using an identical procedure.

Thermogravimetric analysis (TGA)

TGA analyses were carried out using a TA Q5000 thermogravimetric analyser under nitrogen flow (25 ml min^{-1}). Approximately 5 mg of sample was loaded into a platinum HT sample pan, and a dynamic heating method was programmed with 10 °C min^{-1} ramp rate from 25–600 °C. The temperature of decomposition was determined from T_i (initial onset), defined as the initial deviation from the baseline corresponding to the derivative of % weight with respect to temperature.

FT-IR spectroscopy

Attenuated Total Reflectance Fourier-Transform Infrared (ATR-FTIR) spectra were recorded using a PerkinElmer Spectrum Two FT-IR spectrometer equipped with a diamond ATR crystal. Prior to measurement, the ATR accessory was cleaned with ethanol and dried with a lint-free tissue to avoid contamination. Th samples were placed directly onto the diamond crystal with gentle pressure applied via the built-in pressure arm to ensure good contact between the sample and the ATR surface. For each sample, spectra were collected over the range of 4000–400 cm^{-1} with a spectral resolution of 4 cm^{-1}. Each spectrum was averaged over 32 scans to improve the signal-to-noise ratio. Background spectra were collected under the same conditions before

each sample measurement and automatically subtracted from the sample spectra. All measurements were performed at room temperature.

Results and discussion

The objective of this work was to develop a low-cost catalyst for the depolymerisation of polyethylene terephthalate (PET), working under mild conditions and robust enough to withstand contaminated waste feedstocks and blends of polymers. The model catalyst system explored in this work was formulated from triethylamine (N_{222}) and sulfuric acid. It has already been used as a potent and inexpensive catalyst in esterification reactions, and its price was reported to be on par with acetone.[39,40]

Ionic liquid composition

Protic ionic liquids (PILs) can be formulated with an excess of either acid or base, allowing different catalytic mechanisms to be explored within the same ionic framework. In the first set of experiments, PET methanolysis was tested under standard literature conditions (180 °C, 1 h, autogenous pressure, and 0.01 mol catalyst loading). Five catalysts were screened: an equimolar PIL, [HN_{222}][HSO_4]; a basic PIL with a 2 : 1 base : acid ratio, [$HN_{222} \cdot N_{222}$][HSO_4]; an acidic PIL with a 1 : 2 base : acid ratio, [HN_{222}][$HSO_4 \cdot H_2SO_4$]; neat base, N_{222}; and neat acid, H_2SO_4.

The acidic ionic liquid [HN_{222}][$HSO_4 \cdot H_2SO_4$] was excluded from further study due to a rapid increase in pressure above the safety threshold, likely caused by dehydration of methanol to dimethyl ether. Interestingly, this issue was not observed with neat H_2SO_4, demonstrating how modifying a Brønsted acid into an acidic ionic liquid can significantly alter the reaction pathway.

Among the remaining catalysts, the basic ionic liquid [$HN_{222} \cdot N_{222}$][HSO_4] consistently delivered the highest DMT yields. Its improved performance is attributed to increased basicity and reduced acidity. In contrast, the more acidic [HN_{222}][HSO_4] exhibited lower activity. Under acidic conditions, the reaction proceeds via protonation of the ester carbonyl, followed by methanol attack. However, high acidity reduces methanol nucleophilicity and increases viscosity and ionic strength, which limits PET interaction and slows reaction kinetics (Fig. 1).

In the base-rich [$HN_{222} \cdot N_{222}$][HSO_4], triethylamine may partially deprotonate methanol to generate methoxide in situ, which acts as a stronger nucleophile. This promotes PET bond cleavage via a tetrahedral intermediate. While neat triethylamine can initiate this pathway, its volatility, lack of ionic structure, and poor PET solubility limit its practical application. Combining it with sulfuric acid to form an ionic liquid provides thermal and chemical stability, a polar ionic medium for better PET interaction, and reduced volatility.

The acidity of the PILs was quantified via the Gutmann Acceptor Number: [HN_{222}][$HSO_4 \cdot H_2SO_4$] had the highest value (118.46 AN), followed by [HN_{222}][HSO_4] (107.93 AN) and
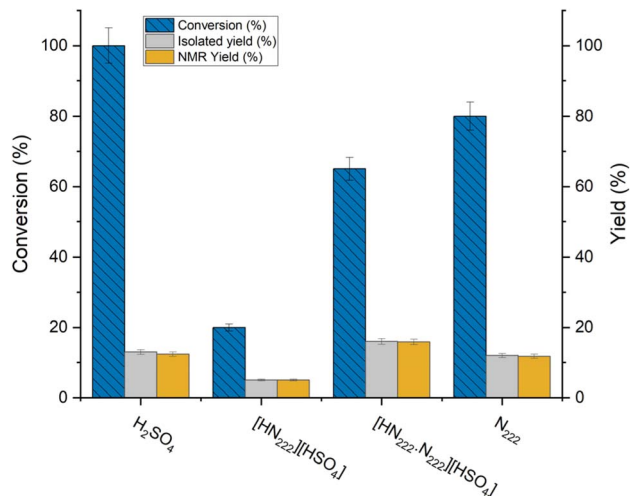
Fig. 1 Conversion (%) of PET and the yield (%) of DMT using a variation of catalysts ranging from acidic to basic. Reaction conditions: PET (0.005 mol), catalysts (0.01 mol), methanol (0.15 mol) and a reaction temperature of 180 °C for 1 h. All reactions were carried out in triplicate.

Fig. 2 Conversion (%) of PET and the yield (%) of DMT using a variation of catalysts ranging from acidic to basic. Reaction conditions: PET (0.002 mol), catalysts (0.01 mol), methanol (0.15 mol) and a reaction temperature of 180 °C for 1 h. All reactions were carried out in triplicate.

$[HN_{222} \cdot N_{222}][HSO_4]$ (20.62 AN). Lower acidity correlated with higher DMT yields, supporting a mechanistic distinction between acid- and base-driven catalysis. These structural and mechanistic factors together explain both the superior performance of the excess base formulation and the enhanced activity of the ionic liquid compared to triethylamine alone.

PET : methanol ratios

Each catalyst was tested under two PET : methanol molar ratios: a low excess of methanol (1 : 30), which is desirable for reduced solvent volume and lower CAPEX, and a high excess (1 : 75), which is more common in the literature for optimised depolymerisation.

At low methanol excess (1 : 30), reactions catalysed by H_2SO_4 and N_{222} showed high PET conversion (100% and 80%, respectively), but low selectivity to DMT (14% and 12%). The equimolar PIL $[HN_{222}][HSO_4]$ had low activity (20% PET conversion, <10% DMT yield), while the basic PIL $[HN_{222} \cdot N_{222}]$ $[HSO_4]$ gave moderate conversion (65%) and slightly better DMT yield (18%). Across all catalysts, DMT selectivity was poor, with most PET converted to TPA, as indicated by GC-MS (Fig. S3). This highlights the challenge of driving the reaction towards DMT formation at lower methanol concentrations.

To improve DMT selectivity, reactions were repeated at a higher methanol excess (1 : 75). This increased PET conversion and DMT yields across all catalysts. N_{222} gave full PET conversion, while others reached 80%. DMT yields improved significantly, ranging from 40–70%, with the highest selectivity (57–86%) observed for $[HN_{222} \cdot N_{222}][HSO_4]$.

This improvement is consistent with Le Chatelier's principle: increasing the concentration of methanol shifts the equilibrium towards DMT and EG, limiting repolymerisation. Excess methanol also helps suppress MHET formation by competing with EG and water as nucleophiles. Although higher methanol
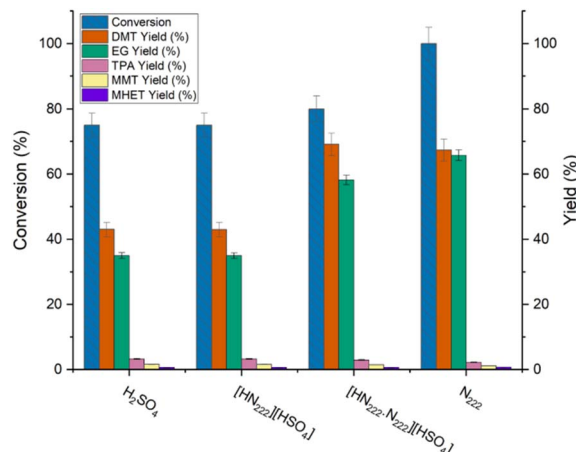
loading increases downstream recovery costs, it clearly enhances product selectivity and conversion efficiency under these conditions (Fig. 2).[41]

Reaction temperature

Optimising temperature and reaction time is key to maximising the yield of DMT while minimising by-products.[42] An optimal methanolysis temperature is known to be around 160–200 °C.[25,34,43] While higher reaction temperature promotes better DMT yields, lower temperature is more cost-effective and associated with lower energy consumption (Fig. 3).

In this work, PET methanolysis was studied within the temperature range of 100–180 °C (Fig. 5), in a reaction catalysed by $[HN_{222} \cdot N_{222}][HSO_4]$, which exhibits the highest selectivity towards DMT. At 100 °C, no products were detected after 1 h. At 120 °C and 140 °C, both conversion and DMT yield remained
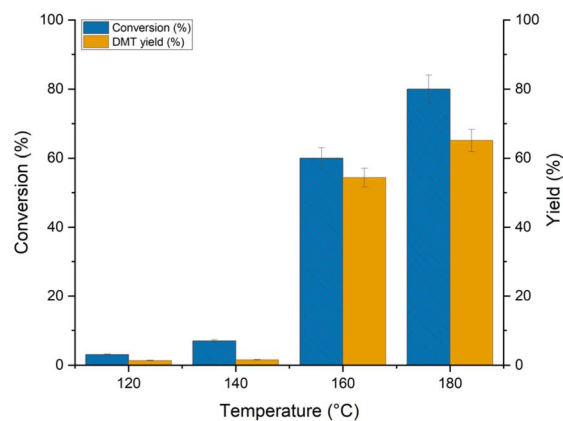
Fig. 3 Effect of temperature on conversion (%) and DMT yield (%). Reaction conditions: PET (0.002 mol) $[HN_{222} \cdot N_{222}][HSO_4]$ (0.01 mol), methanol (0.15 mol) and a reaction temperature of 120–180 °C for 1 h. All reactions were carried out in triplicate.

under 10%. Only at 160 °C, PET conversion reached 60%, and DMT yield reached 54%, with very good selectivity (90%). Further increase in temperature to 180 °C gave satisfactory conversion (85%) and DMT yield (70%), but selectivity to DMT dropped to 81%. A reaction at 200 °C failed due to the generated pressure exceeding the safety threshold of the microwave. As such, a reaction temperature of 180 °C was selected as offering sufficiently high conversion within 1 h, without significantly compromising selectivity.

Reaction time

Methanolysis of PET at 180 °C, catalysed by $[HN_{222} \cdot N_{222}][HSO_4]$, was studied as a function of reaction time (0.25 to 6 h). Experiments were carried out at two PET : methanol molar ratios; 1 : 30 (Fig. 4) and 1 : 75 (Fig. 5).

At the lower ratio (1 : 30), the yield of DMT was analysed by qNMR spectroscopy in the post-reaction mixture and compared to the isolated yield of the crystallised product (Fig. 4). It was possible to quantitatively separate pure DMT in the form of colourless crystals. The isolated yield of DMT reached a plateau at 30% after 2 h, despite a steady rise in conversion up to 6 h.

At the higher methanol excess (1 : 75), it was impossible to quantify isolated yields in a reproducible manner, because increased volume of methanol with the constraint of fixed volume of the microwave reactor resulted in small absolute quantities of the product. Instead, the reaction progress was followed by GC-MS, enabling quantitative analysis of both DMT and the side products (Fig. 4). At higher methanol excess, conversion of PET reached 80% within 1 h and 100% after 3 h. The main product was DMT, reaching 98% yield after 3 h. For longer reaction times, the yield of DMT dropped due to hydrolysis to TPA, transesterification to MHET and several other side reactions. It is known that extended reaction times result in the degradation of EG to acetaldehydes, glycolic acid or formic acid.[44] Furthermore, it allows the formation of oligomers that

Fig. 5 Effect of reaction time on PET depolymerisation with conversion (%) (blue), DMT yield (%) (orange), TPA yield (%) (pink), MHET yield (%) (green) and MMT yield (%) (purple) measured by GC-MS. Reaction conditions: PET (0.002 mol) $[HN_{222} \cdot N_{222}][HSO_4]$ (0.01 mol), methanol (0.15 mol) and a reaction temperature of 180 °C. All reactions were carried out in triplicate.

are not detected by GC-MS, as they precipitate out during the derivatisation of the GC-MS sample.

In conclusion, while it was not feasible to reach satisfactory yields of DMT using the low methanol excess, it was possible to reach full conversion of PET to DMT at high methanol excess, under reaction conditions on par with the literature (Table 1), but using an ionic liquid catalyst that is as cheap as acetone.[36]

Reusability of the IL catalyst

To evaluate the reusability of the ionic liquid catalyst $[HN_{222} \cdot N_{222}][HSO_4]$, five consecutive methanolysis cycles were performed under both high and low PET : methanol molar ratio conditions. These studies allowed for direct comparison of catalyst performance, product recovery, and side-product accumulation under varying operational challenges. Under high methanol excess, mass balance results showed consistent material recovery and minimal loss over five cycles (Tables S1 and S2). DMT recovery remained stable (0.45–0.49 g per cycle), and the ionic liquid mass varied by less than 0.1 g between cycles, indicating high catalyst retention, expected to further improve upon scale-up. Ethylene glycol levels were consistent, and no significant accumulation of side products was observed (Fig. S28, ^{1}H and ^{13}C NMR spectra of isolated ethylene glycol). In conclusion, the ionic liquid remains catalytically active and chemically stable across multiple uses, where excess methanol suppresses side reactions and facilitates clean phase separations. Under the more demanding low methanol condition, mass balance trends indicated slightly higher material losses and more pronounced accumulation of by-products (Table S2). DMT yields were consistent (0.35–0.37 g), though slightly lower than in the high-ratio system, which may reflect increased competition from side reactions. The recovered ionic liquid mass gradually declined from 3.50 g to 3.04 g over five cycles, as expected at this small scale (Fig. 6).
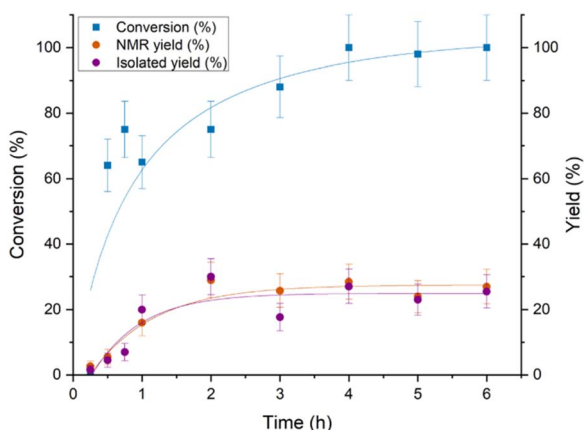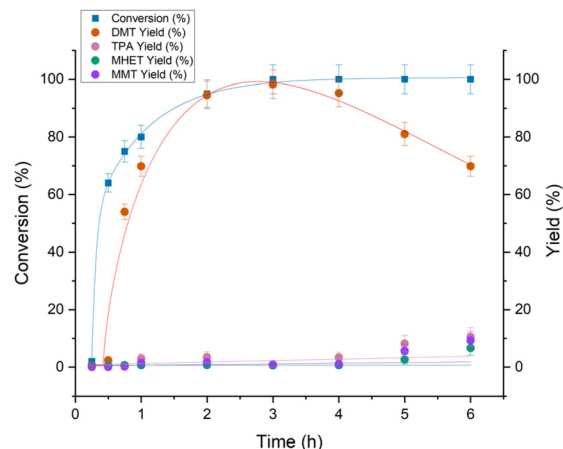

Fig. 4 Effect of reaction time on PET depolymerisation with conversion (%) (blue), isolated yield (%) (purple) and NMR yield (%) (orange) measured. Reaction conditions: PET (0.005 mol) $[HN_{222} \cdot N_{222}][HSO_4]$ (0.01 mol), methanol (0.15 mol) and a reaction temperature of 180 °C. All reactions were carried out in triplicate.
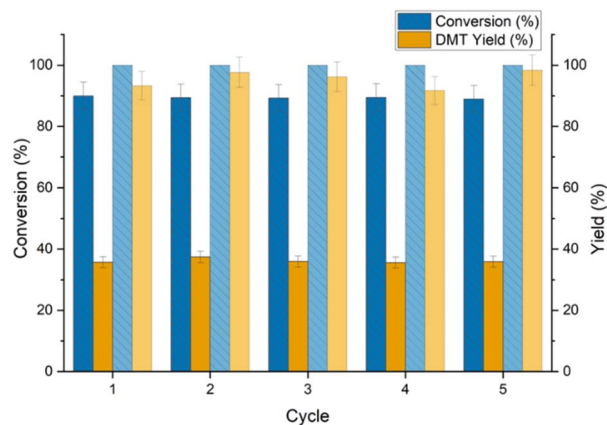
Fig. 6 The reusability cycle of $[HN_{222}\cdot N_{222}][HSO_4]$ on the conversion (%) and DMT yield (%). Reaction conditions: PET (0.005 mol) $[HN_{222}\cdot N_{222}][HSO_4]$ (0.01 mol), methanol (0.15 mol) (dark blue and orange). PET (0.0025 mol) $[HN_{222}\cdot N_{222}][HSO_4]$ (0.01 mol), methanol (0.15 mol) (light blue and orange) and a reaction temperature of 180 °C for 3 h.

Using a high methanol ratio offers sustained catalytic performance, cleaner product recovery, and minimal interference from side-product formation. In contrast, the low methanol excess was used to ensure a more rigorous test of catalyst robustness, revealing the limitations imposed by increasing concentrations of EG and other side products, which were extracted by ethyl acetate (Fig. S29 and S30, ^{1}H and ^{13}C NMR spectra of the organic layer). These may reduce isolated DMT yields through transesterification or other secondary reactions. In conclusion, using higher methanol excess is recommended in practice to maximise catalyst lifetime and reduce waste processing burdens in future scale-up applications.

Robustness of the catalyst against complex PET waste

While PET bottles are, to an extent, recycled mechanically, recycling highly coloured and blended PET waste remains much more challenging. Currently, about 30% of PET bottles are recycled, with 75% being rejected. Of the 25% that is recycled, 17% is returned to bottle production, while 50% is blended into fibres for products such as sports garments or carpets.[1-3] This creates a significant problem: although PET is perceived as a recyclable polymer, most recycled bottles are diverted into non-recyclable applications, extending the supply chain in

a linear economy rather than promoting a circular one. Additionally, this process can mislead consumers with "green" credentials, as the materials cannot be recycled in the same way.

The key test for the $[HN_{222}\cdot N_{222}][HSO_4]$ catalyst was its robustness against more challenging PET waste, in the form of a carpet sample containing dyed PET fibres with a latex backing (Fig. 7). Methanolysis of carpet samples was carried out by cutting them into small pieces using scissors and placing them on a balance. The latex backing was removed from the PET strands to weigh the quality of PET. The PET was combined with the latex backing and placed in the reaction vessel. The reaction was carried out under optimised conditions (180 °C, 3 h, high excess of methanol). The isolated yield was calculated based on the starting moles of PET and measured using GC-MS.

Methanolysis of carpet waste under the conditions optimised for PET bottles gave 100% conversion of the PET fibres and a 97% isolated yield of DMT. It has been determined that the presence of dyes and the latex backing did not inhibit the depolymerisation reaction or reduce product yield, which is an important advantage for practical applications in chemical recycling. The latex backing remained intact post-reaction and was easily separated (Fig. 7), in contrast to many other ionic liquids that degrade latex,[45] which would complicate the separation and purification of DMT. GC-MS analysis showed no detectable dyes in the spectrum, and the purity of the DMT was determined by NMR using 1,3,5-trimethoxybenzene as an internal standard, resulting in a purity of 98% (Fig. S31 and S32) While some dye accumulation in $[HN_{222}\cdot N_{222}][HSO_4]$ may occur over time and require periodic removal, detailed analysis of dye contamination and its long-term effects was beyond the scope of this study. Nevertheless, catalytic performance appeared unaffected, indicating the ionic liquid catalyst's tolerance to such additives. Unlike the findings reported by Muangmeesri *et al.*, where yield decreased significantly upon introducing a mixed feedstock,[32] the use of ionic liquids in this study offers the advantage of maintaining higher yields despite feedstock complexity.

Conclusions

An inexpensive, protic ionic liquid, $[HN_{222}\cdot N_{222}][HSO_4]$, was used as an effective catalyst for the methanolysis of PET from waste water bottles and mixed carpet fibres under microwave irradiation. The overall performance in terms of reaction conditions and yield of DMT matches literature methods reported for PET bottles. This process offers several advantages. In contrast to most systems compared in Table 1, $[HN_{222}\cdot N_{222}][HSO_4]$ is very cheap and synthesised in one step from commodity chemicals. Furthermore, it has been demonstrated that the catalyst performs equally well against the standard feedstock of PET from plastic bottles (ground to a fine powder in a ball mill) and against roughly cut carpet. Finally, efficient separation of clean, crystalline DMT is possible by crystallisation directly from the reaction mixture, simplifying downstream processing. These combined benefits highlight the potential of this method as a scalable and economically viable alternative for chemical recycling of PET waste.
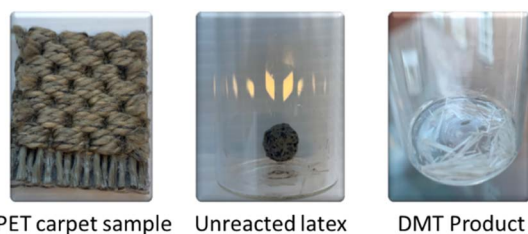

Fig. 7 Visual representation of the PET carpet and the end results. Unreacted latex was separated from the DMT product.

Conflicts of interest

There are no conflicts to declare.

Data availability

The data supporting this article have been included as part of the SI.

The supplementary information provides ^{13}C, ^{1}H, ^{31}P, and qNMR spectra, GC-MS chromatograms with calibration curves, TGA analyses, and a mass balance table supporting the findings of this study. See DOI: https://doi.org/10.1039/d5su00316d.

Acknowledgements

References

1 H. Lamb and S. Defruyt, *The UK Plastics Pact Annual Report, 2022-2023*, 2022.

2 *Redesigning the plastics system – the role of non-mechanical recycling*, https://wrap.org.uk/sites/default/files/2022-08/Redesigningtheplasticssystem-theroleofnon-mechanicalrecycling.pdf, accessed 11 March 2025.

3 *Non-technical challenge to non-mechanical recycling*, https://wrap.org.uk/sites/default/files/2022-08/Non-TechnicalChallengestoNon-MechanicalRecycling.pdf, accessed 11 March 2025.

4 R. Salas, R. Villa, F. Velasco, F. G. Cirujano, S. Nieto, N. Martin, E. Garcia-Verdugo, J. Dupont and P. Lozano, *Green Chem.*, 2025, **27**, 1620–1651.

5 M. Wang, Y. Li, L. Zheng, T. Hu, M. Yan and C. Wu, *Polym. Chem.*, 2024, **15**, 585–608.

6 D. Bura, L. Pedrini, C. Trujillo and S. J. Connon, *RSC Sustainability*, 2023, **1**, 2197–2201.

7 Z. Ju, W. Xiao, X. Lu, X. Liu, X. Yao, X. Zhang and S. Zhang, *RSC Adv.*, 2018, **8**, 8209–8219.

8 L. Wang, G. A. Nelson, J. Toland and J. D. Holbrey, *ACS Sustain. Chem. Eng.*, 2020, **8**, 13362–13368.

9 C. Shuangjun, S. Weihe, C. Haidong, Z. Hao, Z. Zhenwei and F. Chaonan, *J. Therm. Anal. Calorim.*, 2021, **143**, 3489–3497.

10 Q. F. Yue, L. F. Xiao, M. L. Zhang and X. F. Bai, *Polymers*, 2013, **5**, 1258–1271.

11 G. S. Ha, M. Al Mamunur Rashid, J. M. Ha, C. J. Yoo, B. H. Jeon, K. Jeong and K. H. Kim, *Chemosphere*, 2024, **349**, 140781.

12 N. G. Bush, C. H. Dinh, C. L. Catterton and M. E. Fieser, *RSC Sustainability*, 2023, **1**, 938–947.

13 D. Thomas, R. Ranjan and B. K. George, *RSC Sustainability*, 2023, **1**, 2277–2286.

14 J. Jonathan, R. Arias and W. Thielemans, *Green Chem.*, 2021, **23**, 9636–9648, DOI: 10.1039/d1gc02896k.

15 T. Yoshioka, T. Motoki and A. Okuwaki, *Ind. Eng. Chem. Res.*, 2000, **39**, 1171–1176, DOI: 10.1021/ie000592u.

16 M. Rollo, M. A. G. Perini, A. Sanzone, L. Polastri, M. Tiecco, A. Torregrosa-Chinillach, E. Martinelli and G. Ciancaleoni, *RSC Sustainability*, 2023, **2**, 187–196.

17 M. Rollo, M. A. G. Perini, A. Sanzone, L. Polastri, M. Tiecco, A. Torregrosa-Chinillach, E. Martinelli and G. Ciancaleoni, *RSC Sustainability*, 2024, **2**, 187–196.

18 M. Azeem, O. A. Attallah, C. E. Tas and M. B. Fournet, *J. Polym. Environ.*, 2024, **32**, 303–315.

19 H. Gruschke, W. Hammerschick and H. Medem, *US Pat.*, US3403115A, 1968.

20 A. Naujokas, *EP Pat.*, EP0857714A1, 1998.

21 R. Francis, *Recycling of Polymers: Methods, Characterization and Applications*, John Wiley & Sons, 2016.

22 C. S. Nunes, M. J. Vieira da Silva, D. Cristina da Silva, A. dos R. Freitas, F. A. Rosa, A. F. Rubira and E. C. Muniz, *RSC Adv.*, 2014, **4**, 20308–20316.

23 H. Kurokawa, M. A. Ohshima, K. Sugiyama and H. Miura, *Polym. Degrad. Stab.*, 2003, **79**, 529–533.

24 M. Ma, S. Wang, Y. Liu, H. Yu, S. Yu, C. Ji, H. Li, G. Nie and S. Liu, *J. Appl. Polym. Sci.*, 2022, **139**, 1–12.

25 J. Tang, X. Meng, X. Cheng, Q. Zhu, D. Yan, Y. J. Zhang, X. Lu, C. Shi and X. Liu, *Ind. Eng. Chem. Res.*, 2023, **62**, 4917–4927.

26 R. Sharpe and M. Morrow, *World Pat.*, WO2021/126661Al, 2021.

27 S. Tang, F. Li, J. Liu, B. Guo, Z. Tian and J. Lv, *J. Chem. Technol. Biotechnol.*, 2022, **97**, 1305–1314.

28 D. D. Pham and J. Cho, *Green Chem.*, 2021, **23**, 511–525.

29 M. Hofmann, J. Sundermeier, C. Alberti and S. Enthaler, *ChemistrySelect*, 2020, **5**, 10010–10014.

30 M. Imran, D. H. Kim, W. A. Al-Masry, A. Mahmood, A. Hassan, S. Haider and S. M. Ramay, *Polym. Degrad. Stab.*, 2013, **98**, 904–915.

31 V. Vinitha, M. Preeyanghaa, M. Anbarasu, B. Neppolian and V. Sivamurugan, *Environ. Sci. Pollut. Res.*, 2023, **30**, 75401–75416.

32 S. Muangmeesri, K. R. Baddigam, K. Navare, V. Apostolopoulou-Kalkavoura, K. Witthayolankowit, H. Håkansson, A. P. Mathew, K. Van Acker and J. S. M. Samec, *ACS Sustain. Chem. Eng.*, 2024, **12**, 4114–4120.

33 Z. Jiang, D. Yan, J. Xin, F. Li, M. Guo, Q. Zhou, J. Xu, Y. Hu and X. Lu, *Polym. Degrad. Stab.*, 2022, **199**, 109905.

34 J. Li, D. Yan, X. Cheng, C. Rong, J. Feng, X. Feng, J. Xin, Q. Zhou, Y. Li, J. Xu and X. Lu, *Ind. Eng. Chem. Res.*, 2024, **63**, 12373–12384.

35 A. S. Amarasekara, J. A. Gonzalez and V. C. Nwankwo, *J. Ionic Liq.*, 2022, **2**, 100021.

36 A. George, A. Brandt, K. Tran, S. M. S. N. S. Zahari, D. Klein-Marcuschamer, N. Sun, N. Sathitsuksanoh, J. Shi, V. Stavila, R. Parthasarathi, S. Singh, B. M. Holmes, T. Welton, B. A. Simmons and J. P. Hallett, *Green Chem.*, 2015, **17**, 1728–1734.

37 A. McGrogan, E. L. Byrne, R. Guiney, T. F. Headen, T. G. A. Youngs, A. Chrobok, J. D. Holbrey and M. Swadźba-Kwaśny, *Phys. Chem. Chem. Phys.*, 2023, **25**, 9785–9795.

38 A. Brzęczek-Szafran, K. Erfurt, M. Swadźba-Kwaśny, T. Piotrowski and A. Chrobok, *ACS Sustain. Chem. Eng.*, 2022, **10**, 13568–13575.

39 A. Brzęczek-Szafran, J. Więcławik, N. Barteczko, A. Szelwicka, E. Byrne, A. Kolanowska, M. Swadźba Kwaśny and A. Chrobok, *Green Chem.*, 2021, **23**, 4421–4429.

40 L. Chen, M. Sharifzadeh, N. Mac Dowell, T. Welton, N. Shah and J. P. Hallett, *Green Chem.*, 2014, **16**, 3098–3106.

41 M. M. Lawal, T. Govender, G. E. M. Maguire, H. G. Kruger and B. Honarparvar, *Int. J. Quantum Chem.*, 2022, **118**, e25497, DOI: **10.1002/qua.25497**.

42 J. Tang, X. Meng, X. Cheng, Q. Zhu, D. Yan, Y. J. Zhang, X. Lu, C. Shi and X. Liu, *Ind. Eng. Chem. Res.*, 2023, **62**, 4917–4927.

43 T. Uekert, A. Singh, J. S. DesVeaux, T. Ghosh, A. Bhatt, G. Yadav, S. Afzal, J. Walzberg, K. M. Knauer, S. R. Nicholson, G. T. Beckham and A. C. Carpenter, *ACS Sustain. Chem. Eng.*, 2023, **11**, 965–978.

44 L. Ye, L. Zhao, L. Zhang and F. Qi, *J. Phys. Chem. A*, 2012, **116**, 55–63.

45 J. Lu, Y. Ding, Y. Yu, S. Wu and W. Feng, *Macromol. Symp.*, 2010, **298**, 167–173.